NUMERICAL INVESTIGATION OF INSULATION EFFECT ON SOLAR POND

I. Bozkurt[a,]* H. Sogukpinar[b] M. Karakilcik[c] H. Turkmenler[d] M. Pala[e]
[a]Department of Mechanical Engineering, Faculty of Engineering, University of Adiyaman, Turkey
[b]Energy Systems Engineering, Faculty of Technology, University of Adiyaman, Turkey
[c]Department of Physics, Faculty of Sciences and Letters, University of Cukurova, Adana, Turkey
[d]Department of Environmental Engineering, Faculty of Engineering, University of Adiyaman, Turkey
[e]Department of Civil Engineering, Faculty of Engineering, University of Adiyaman, Turkey
*E-mail address:ibozkurt@adiyaman.edu.tr

Received date: October 2015
Accepted date: November 2015

Abstract

Solar energy is one of the most important renewable energy sources. Solar heat generation is widely used. Solar pond collects and stores solar energy in the form of heat. Solar pond consists of layers of different density from top to bottom. Salt gradient in the solar pond prevents heat loss by convection in this structure. As well as the heat losses from side and bottom walls are very important to minimize heat losses. In this study, insulated and non-insulated solar ponds were modeled at the same dimensions and summer months. The temperature distributions of the solar pond were obtained during three months (e.g. June, July, August). Furthermore, the temperature distributions were compared for insulated and non-insulated solar ponds. According to calculations, insulated solar pond was found to be much more efficient.

Keywords: Solar energy, solar pond, temperature distribution

1. Introduction

Turkey has high solar energy potential because of its location in the northern hemisphere with latitudes 36–42^0 N and longitudes 26–45^0 E [1]. The greatest advantage of solar energy as compared with other forms of renewable energy is that it is clean and can be supplied without environmental pollution [2]. One of the useful solar energy systems is solar pond. Its main advantage is to prevent convection heat losses by dissolving salt into the bottom layer of this pond, making it too heavy to rise to the surface, even when hot [3]. Solar ponds have many advantages such as economic, simple structure and long-term heat storage features. In this regard, many studies on solar ponds have been done experimentally and theoretically. Bozkurt et. al. [4-6] studied on different types solar ponds to figure out the energy and exergy evaluation. In these studies, the effect of the transparent covers and solar collectors on solar ponds were examined. Karakilcik et. al. [7] investigated the solar pond performance with and without shading effect, the exergetic performance of a solar pond, the temperature and performance distributions in an insulated solar pond. Ranjan et. al. [8] reviewed the solar pond technologies, its thermodynamic and economic feasibility. It was found that this system is useful for low heat applications. Kurt et. al. [9] investigated experimentally and theoretically whether sodium carbonate salt is suitable for establishing a salinity gradient in a salt-gradient solar pond. It was found that a considerable amount of solar energy can be trapped and stored as heat energy in heat storage zone of the pond. Karakilcik et. al. [10] investigated experimental and theoretical of temperature distributions in an insulated solar pond, particularly during daytimes and night times, for Adana, Turkey. In the model, the temperature distributions were calculated for the three zones of the insulated solar pond. Kayali et. al. [11] investigated a mathematical model of a rectangular solar pond to determine the temperature distribution of the solar pond for the Cukurova region of Turkey. One and two-dimensional heat balance equations were written. In addition, using meteorological data, empirical functions for ambient air and soil temperatures were developed.

In this study, insulated and non-insulated solar ponds were modeled at the same dimensions and summer months for Adiyaman climatic conditions, Turkey. The temperature distributions of the solar pond were obtained during three months (e.g. June, July, August). Furthermore, the temperature distributions were compared for insulated and non-insulated solar ponds.

2. Description of solar pond

Solar pond consists of three zones. The density of the zones increases with depth. The surface zone is called as Upper Convective Zone (UCZ). UCZ is formed fresh water. The middle zone is called as Non-Convective Zone (NCZ) and it is formed layers with different density. These layers prevent heat loss by convection. The bottom zone is called as Heat Storage Zone (HSZ) and it is formed with salty water with high density. An amount of solar radiation reaching the surface of the solar pond is reflected by the surface. The rest radiation is transmitted to NCZ. A small amount of radiation is absorbed by UCZ and NCZ. The most of the solar radiation is transmitted to HSZ and. the majority of solar energy is absorbed and stored in HSZ. Very little is reflected by the bottom of the pond. In this study, two solar ponds 2 m x 2 m x 1.5 m in size were investigated. One of them is insulated with 0.10 m thickness foam, and the other is designed to be un-insulated. As shown in Fig. 1, layers comprising both ponds were modeled as having the same density and same thickness.

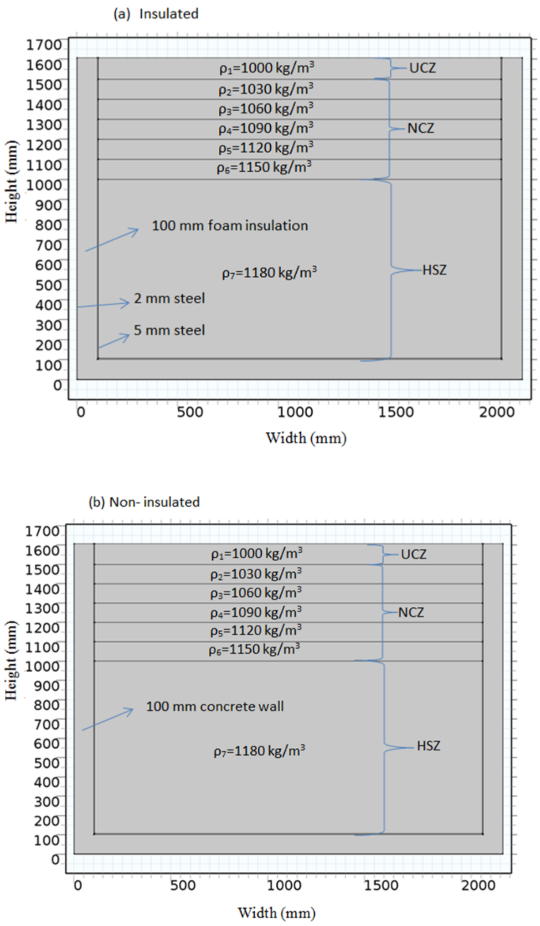

Figure 1: Computational domain for insulated and non-insulated condition and boundary requirement

3. Modeling of the system

Heat transfer is defined as movement of energy from one place to another depending on the temperature difference in mediums. Heat transfer takes place in three different ways these are conduction, convection and radiation. Heat transfer takes place according to the first law of thermodynamics, commonly referred to as the principle of conservation of energy. Basic law is usually rewritten in terms of temperature to solve heat transfer equation and is expressed with the equation (1) [12-13]:

$$\rho C_p\left(\frac{\partial T}{\partial t}+(u.\nabla)T\right)=-\nabla.(q_c+q_r)+\tau{:}\mathrm{S}-\frac{T}{\rho}\frac{\partial \rho}{\partial T}\Big]\left(\frac{\partial p}{\partial t}+(u.\nabla)p\right)+\mathrm{Q}_p \tag{1}$$

Where, ρ is the density (kg/m^3), C_p is the specific heat capacity at constant pressure (J/(kg·K)), T is absolute temperature (K), u is the velocity vector (m/s), q_c and q_r heat flux by conduction and radiation (W/m^2), p is pressure (Pa), τ is the viscous stress tensor (Pa), S is the strain-rate tensor (1/s), Q contains heat sources other than viscous heating (W/m^3) The amount of heat by radiation transferred to the environment is calculated using with the help of equation (2):

$$\Omega.\nabla I(\Omega)=\kappa I_b(T)-\beta I(\Omega)+\frac{\sigma_s}{4\pi}\int_0^4 I(\Omega')\phi(\Omega',\Omega)d\Omega' \tag{2}$$

Where, $I(\Omega)$ is radiation intensity in the Ω direction, T is temperature, κ,β,σ_s absorption, extinction and scattering coefficient respectively, $I_b$is blackbody radiation intensity and Φ is the scattering phase function. In order to treat radiation intensity equation numerically, the angular space is discretized and discrete ordinates method is implemented. Assuming that model is invariant in the z direction and discrete ordinates method in the form of radiative transfer equation in the direction of Ω_{i+} and Ω_{i-} expressed with the help of equation (3) and (4) [12-13]:

$$\Omega_{i+}.\nabla I_{i^+}=\kappa I_b(T)-\beta I_{i^+}+\frac{\sigma_s}{4\pi}\sum_{j=1}^{n}\omega_j I_j\Phi(\Omega_j,\Omega_{i+}) \tag{3}$$

$$\Omega_{i}.\nabla I_{i}=\kappa I_b(T)-\beta I_{i}+\frac{\sigma_s}{4\pi}\sum_{j=1}^{n}\omega_j I_j\Phi(\Omega_j,\Omega_{i}) \tag{4}$$

There are four options to define discretization level and these are Linear, Quadratic, Cubic, and Quartic but for this study linear is preferred. Absorption coefficient and Scattering coefficient are selected as from materials option. For the scattering type, there are three option and these are isotropic, polynomial anisotropic and linear anisotropic. Computational conditions are given in Table 1. For the meshing, physics controlled mesh sequence types is preferred and as element size extremely coarse is chosen because no need to use high size meshing for this domain. Mesh distribution for solar pond is given in Figure 2. Physical domain consists of 7 layers. The bottom layer known as HSZ has depth of 60cm and the other layers have a depth of 10 cm. The density of the brine contained in the layers increases steadily. The first pool has 10 cm thick foam insulation and the other pond is made from 10 cm thick concrete respectively. Computational domain for isolated and non-isolated condition and boundary requirement are given in Figure 1.

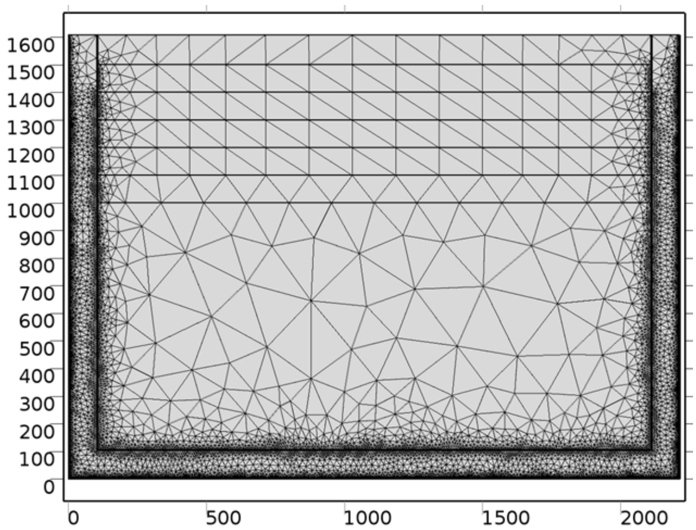

Figure 2: Mesh distribution for solar pond

Table 1. Computational condition

Incident radiation	275.27 W/m^2, 287.62 W/m^2, 258.79 W/m^2
Wall types	Gray
Initial temperature	293.15 K
Outside Temperature	299.8 K, 305.09 K, 305.78 K
Reference pressure	1 atm
Method	Discrete Ordinate methods
Wall height	1600 mm

4. Results and discussion

In this study, we presented the results of the numerical calculations to determine the temperature distribution for insulated and non-insulated solar ponds. In this model, air temperature and incident solar radiation reaching the surface of the pond were used. Temperature distribution of the solar pond is effected by many factors such as insulation materials, air temperature, rainfall and incoming solar energy. Figure 3 shows temperature distribution for insulated solar pond starting from June to August. As seen in Fig. 3, the temperature distribution in UCZ layer remains approximately the same with air temperature because this zone is surface zone. The temperature in NCZ increases with depth similar to the density gradient. The highest temperature is reached in HSZ. HSZ temperature increased rapidly and reached up to 345 K in July. Fig. 4 shows the temperature distribution for non-insulated solar pond starting from June to August. Temperature change in non-insulated solar pond shows similar properties with insulated solar pond. HSZ temperature reached up to 335 K in July for non-insulated solar pond.

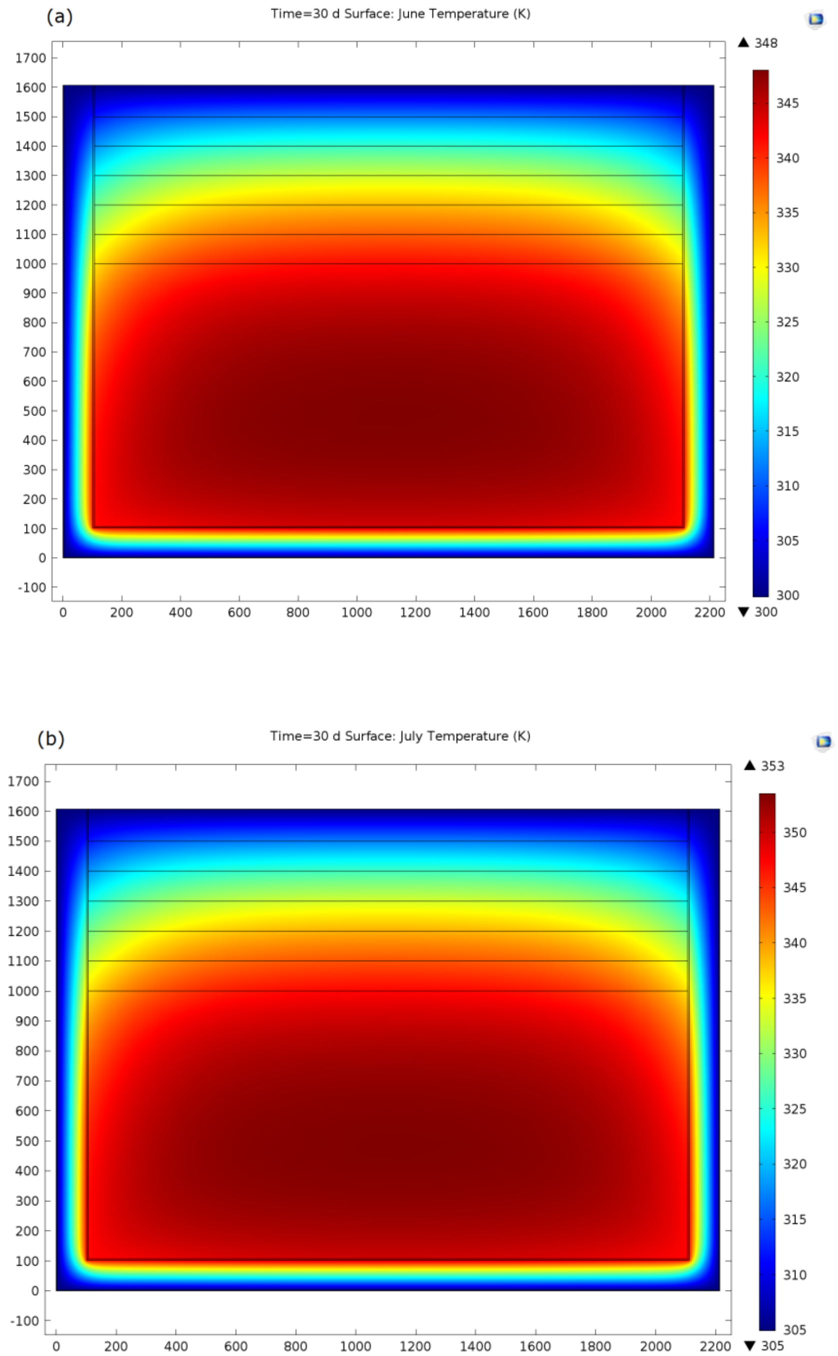
(a)
Time=30 d Surface: June Temperature (K)
▲ 348
▼ 300
(b)
Time=30 d Surface: July Temperature (K)
▲ 353
▼ 305

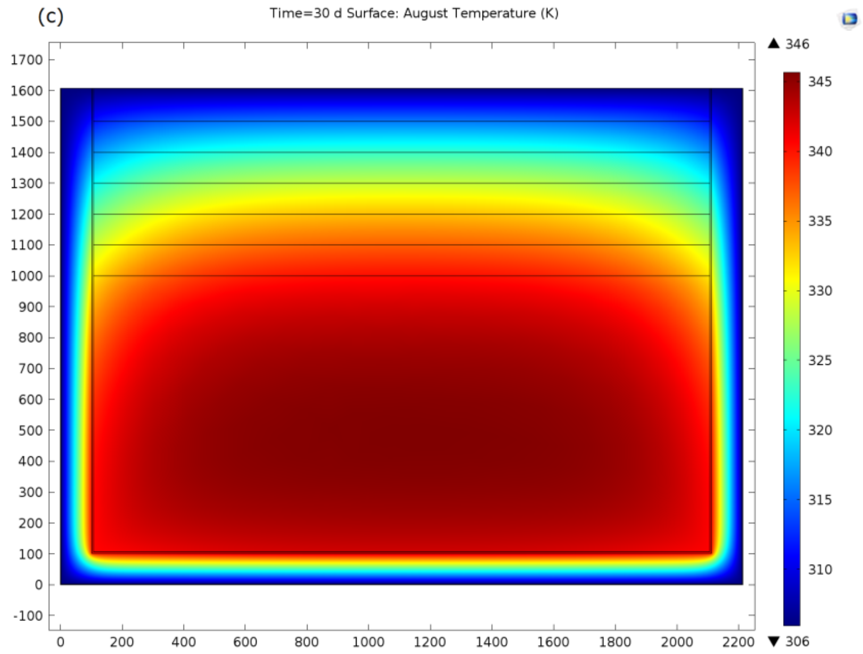

Figure 3: Temperature distribution for insulated solar pond starting from June to August

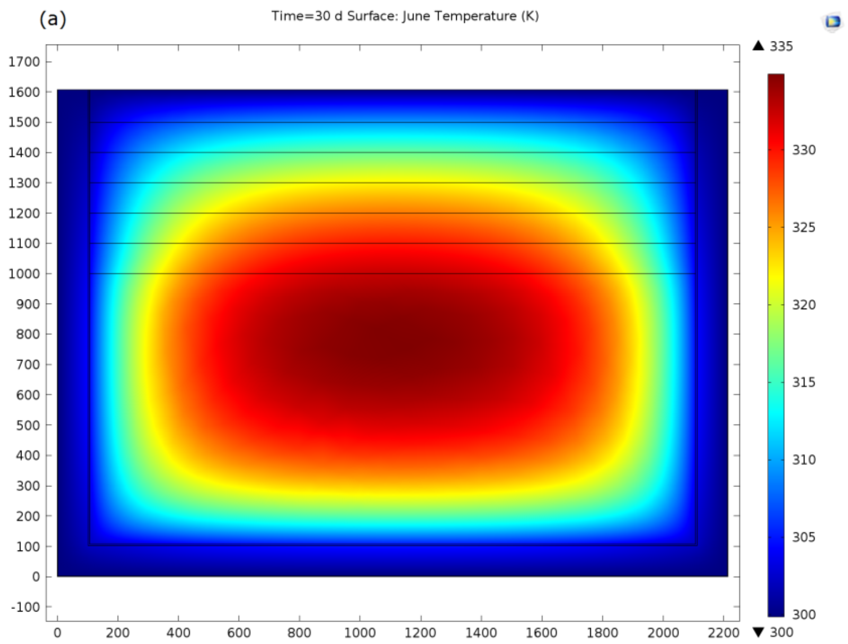

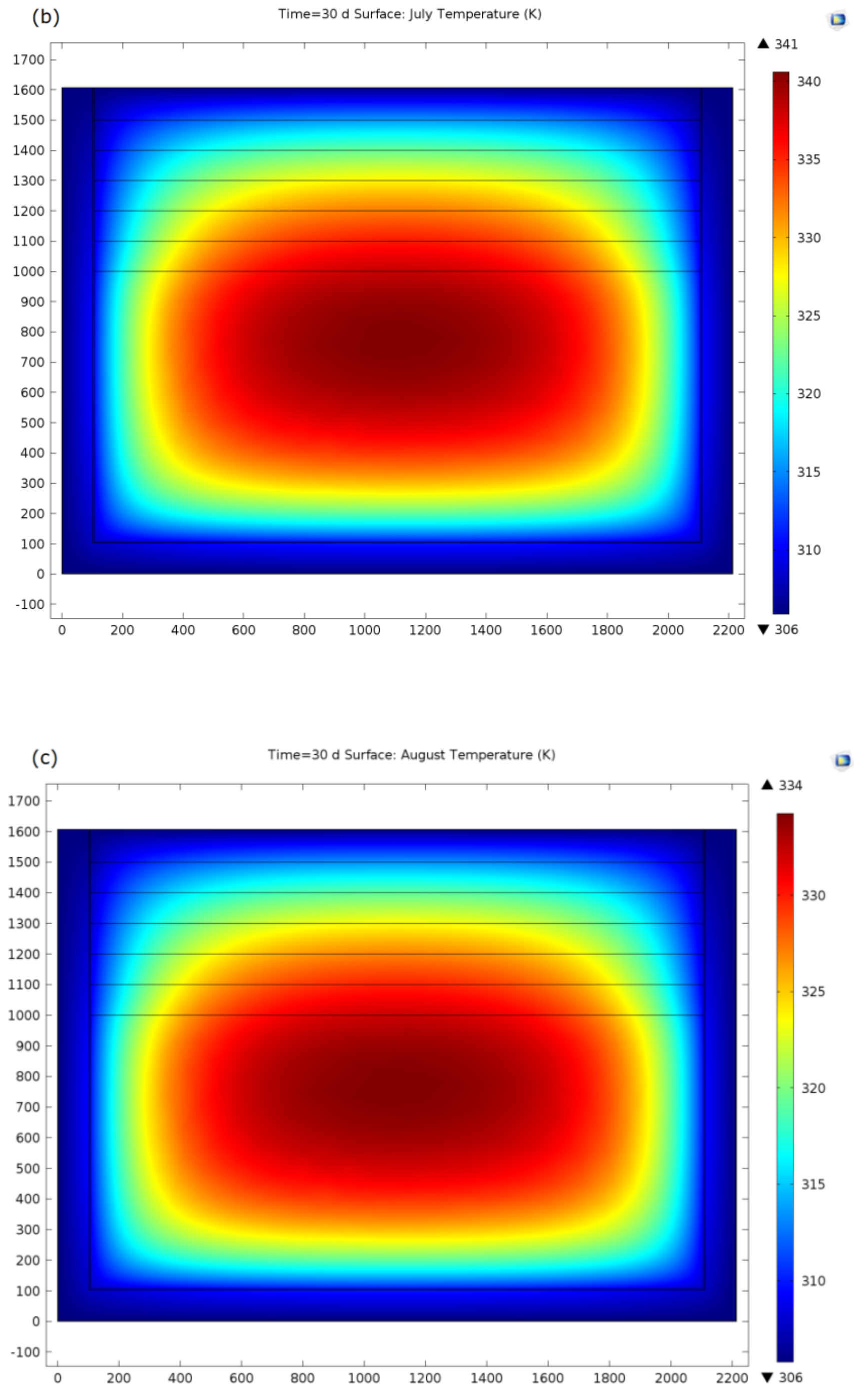

Figure 4: Temperature distribution for non-insulated solar pond starting from June to August

The temperature in the solar pond increases toward the bottom similar to the density gradient. Insulated and non-insulated solar pond temperature distribution for HSZ, NCZ and UCZ are shown in Figure 5. As shown in Fig. 5, it is seen that maximum temperature in HSZ in July with the value of 345 K and 335 K for insulated and non-insulated solar pond, respectively. Furthermore, it is seen that the maximum temperature for July at NCZ with the value of 335 K and 330 K for insulated and non-insulated solar pond, respectively. The maximum temperature in July is observed in UCZ for insulated and non-insulated as 317 K and 315 K respectively.

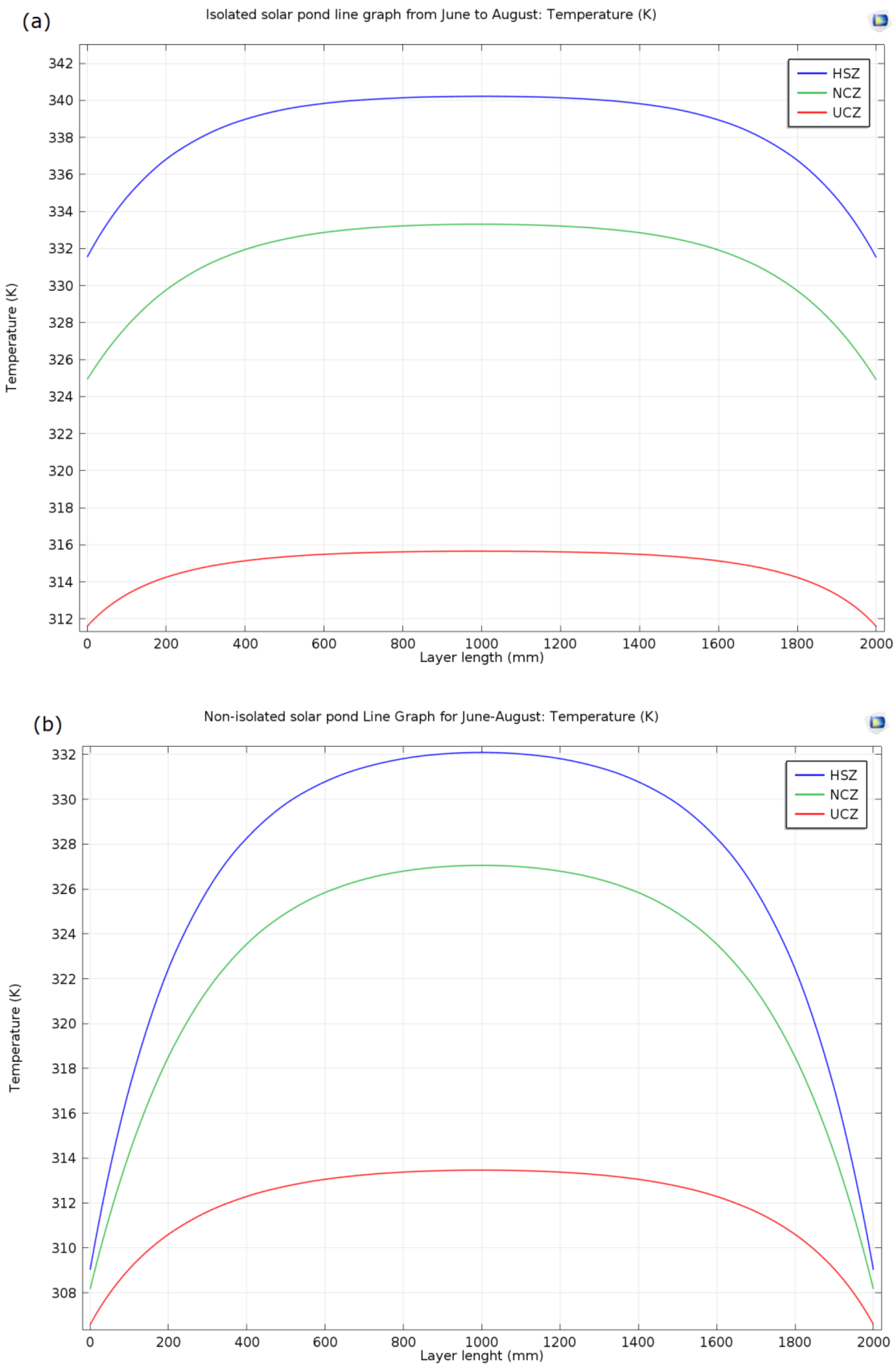

Figure 5: The temperature distribution of the zones for insulated and non-insulated solar pond

5. Conclusion

Solar pond is an important solar energy system with a simple structure and long-term heat storage performance. In this study, we investigated the temperature distribution for insulated and non-insulated solar ponds to determine the effect of insulation. For this purpose, a software program (COMSOL) was used. The air temperature and solar radiations data were taken from Turkish State Meteorological Service for Adiyaman. The temperature distributions in the solar pond depend on different parameters. The most important one is insulation. The temperature distributions of the insulated and non-insulated solar pond in the same size were determined for the three zones of the solar pond at the same climatic condition. As a result, it has been shown that the insulated solar ponds, designed to be insulated using appropriate insulation materials, is found to be more efficient with respect to non-insulated solar pond.

Acknowledgment

I thank Middle East Technical University, allowing me to this work in there with their facility.

Notations

HSZ	Heat storage zone
NCZ	Non-convective zone
UCZ	Upper convective zone
ρ	Density (kg/m^3)
C_p	Specific heat capacity at constant pressure (J/kg·K)
T	Absolute temperature (K)
u	Velocity vector (m/s)
q	Heat flux by conduction (W/m^2)
q_r	Radiative heat flux (W/m^2)
p	Pressure (Pa)
τ	Viscous stress tensor (Pa)
S	Strain-rate tensor (1/s)
Q	Heat sources other than viscous heating (W/m^3)
U	Internal energy (J)
h	Heat transfer coefficient ($W/m^2 \cdot K$).
k	Thermal conductivity of the fluid (W/m·K).
q_0	Inward heat flux (W/m^2)

References

[1] Saylan, L., Sen, O., Toros, H., Arisoy, A., Solar energy potential for heating and cooling systems in big cities of Turkey. *Energy Conversion and Management,* 43, 1829–1837, 2002.

[2] Kalogirou, S.A., Solar Energy Engineering Processes and Systems, 1st Edition. Cyprus University of Technology ISBN 13:978-0-12-374501-9, 2009.

[3] Dincer, I., Rosen, M.A., Thermal Energy Storage Systems and Applications, second ed. Wiley, New York, 2011.

[4] Bozkurt, I., Karakilcik, M., The daily performance of a solar pond integrated with solar collectors. *Solar Energy*, 86, 1611-1620, 2012.

[5] Bozkurt, I., Karakilcik, M., Dincer, I., Atiz, A., Transparent covers effect on the performance of a cylindrical solar pond. *International Journal of Green Energy,* 11, 404–416, 2014.

[6] Bozkurt, I., Karakilcik, M., Dincer, I., Energy efficiency assessment of integrated and nonintegrated solar ponds. *International Journal of Low-Carbon Technologies,* 9, 45–51, 2014.

[7] Karakilcik, M., Dincer, I., Bozkurt, I., Atiz, A., Performance assessment of a solar pond with and without shading effect. *Energy Conversion and Management,* 65, 98–107, 2013.

[8] Ranjan, K.R., Kaushik, S.C., Thermodynamic and economic feasibility of solar ponds for various thermal applications: A comprehensive review. *Renewable and Sustainable Energy Reviews,* 32, 123–139, 2014.

[9] Kurt, H., Ozkaymak, M., Binark, A.K., Experimental and numerical analysis of sodium-carbonate salt gradient solar-pond performance under simulated solar-radiation. *Applied Energy,* 83, 324–342, 2006.

[10] Karakilcik, M., Kıymac, K. and Dincer, I., Experimental and theoretical temperature distributions in a solar pond. *International Journal of Heat and Mass Transfer,* 49, 825–835, 2006.

[11] Kayali, R., Bozdemir, S., Kiymac, K., A rectangular solar pond model incorporating empirical functions for air and soil temperatures. *Solar Energy*, 63, 345–353, 1998.

[12] COMSOL Heat Transfer Module Users Guide. http://www.comsol.com. 2015.

[13] Bozkurt, I., Sogukpinar, H., Karakilcik, M., Modeling of a solar pond for different insulation materials to calculate temperature distribution. *Journal of Multidisciplinary Engineering Science and Technology*, Vol. 2 Issue 6, 1378-1382, 2015.